

Manuscript version: Author's Accepted Manuscript

The version presented in WRAP is the author's accepted manuscript and may differ from the published version or Version of Record.

Persistent WRAP URL:

<http://wrap.warwick.ac.uk/114033>

How to cite:

Please refer to published version for the most recent bibliographic citation information. If a published version is known of, the repository item page linked to above, will contain details on accessing it.

Copyright and reuse:

The Warwick Research Archive Portal (WRAP) makes this work by researchers of the University of Warwick available open access under the following conditions.

Copyright © and all moral rights to the version of the paper presented here belong to the individual author(s) and/or other copyright owners. To the extent reasonable and practicable the material made available in WRAP has been checked for eligibility before being made available.

Copies of full items can be used for personal research or study, educational, or not-for-profit purposes without prior permission or charge. Provided that the authors, title and full bibliographic details are credited, a hyperlink and/or URL is given for the original metadata page and the content is not changed in any way.

Publisher's statement:

Please refer to the repository item page, publisher's statement section, for further information.

For more information, please contact the WRAP Team at: wrap@warwick.ac.uk.

Structural analysis of peptides modified with organo-iridium complexes, opportunities from multi-mode fragmentation

Christopher A. Wootton, Adam J. Millett, Andrea F. Lopez-Clavijo, Cookson K. C. Chiu, Mark P. Barrow, Guy J. Clarkson, Peter J. Sadler, and Peter B. O'Connor*

Received 00th January 2016,
Accepted 00th January 2016

DOI: 10.1039/x0xx00000x

www.rsc.org/

The most widely used anticancer drugs are platinum complexes, but complexes of other transition metals also show promise and may widen the spectrum of activity, reduce side-effects, and overcome resistance. The latter include organo-iridium(III) 'piano-stool' complexes. To understand their mechanism of action, it is important to discover how they bind to biomolecules and how binding is affected by functionalisation of the ligands bound to iridium. We have characterised, by MS and MS/MS techniques, unusual adducts from reactions between 3 novel iridium(III) anti-cancer complexes each possessing reactive sites both at the metal (coordination by substitution of a labile chlorido ligand) and on the ligand (covalent bond formation involving imine formation by one or two aldehyde functions). Peptide modification by the metal complex had a drastic effect on both Collisionally Activated Dissociation (CAD) and Electron Capture Dissociation (ECD) MS/MS behaviour, tuning requirements, and fragmentation channels. CAD MS/MS was effective only when studying the covalent condensation products. ECD MS/MS, although hindered by electron-quenching at the Iridium complex site, was suitable for studying many of the species observed, locating the modification sites, and often identifying them to within a single amino acid residue.

Introduction:

Platinum based metallodrugs are currently used in over 50% of all chemotherapy. They are effective against a wide variety of cancers and have been studied extensively as a result, yielding insights into their mechanisms of action,¹ transformations in solution,² and binding preferences with respect to peptides,³ proteins,⁴ and oligonucleotides.⁵ Unfortunately traditional Pt^{II} drugs, including cisplatin, carboplatin, and oxaliplatin can cause a wide array of side effects and often become less effective during long term treatment when cancerous cells develop resistance to platinum.⁶

Other transition metals show promise as chemotherapy agents, some showing potencies and selectivities exceeding that of cisplatin.⁷ Interestingly these new transition metal complexes exhibit a variety of mechanisms of action.⁸ Some bind to DNA, causing deformations and eventually apoptosis (analogous to cisplatin), other metallodrugs disrupt other vital processes in cells in order to kill target cancer cells, including binding to mitochondria,⁷ or disruption of the NAD⁺/NADH balance inside cells.⁹ Exploring these new mechanisms of action against cancerous cells has become a focus for synthesis of the next generation of anti-cancer compounds.

Unlike the square planar Pt^{II} compounds, some other d-block metal ions readily adopt an octahedral coordination geometry. Pseudo-octahedral 'piano-stool' organo-metallic anti-cancer complexes can be particularly potent for a wide variety of metals, including: ruthenium,¹⁰ rhodium,^{11,12} iridium,^{13,14} and recently osmium.^{7,15}

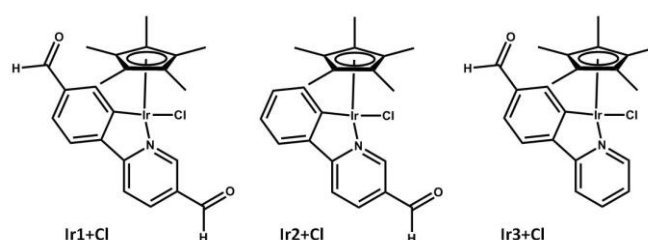


Figure 1: Iridium(III) 'piano-stool' complexes used in this study. The C,N-chelated ligand is functionalized with one (Ir2+Cl, Ir3+Cl) or two (Ir1+Cl) aldehyde groups.

Here we investigate the products formed from reactions of three active¹³ Cp* iridium(III) complexes with the 11-residue peptide Substance P and the 14-residue peptide Bombesin. The three iridium complexes each possess two types of peptide binding sites: the Ir(III) itself, which possesses a labile monodentate chloride ligand that can be substituted by peptide donor atoms (e.g. thioether S of Met and imidazole N of His), together with aldehyde substituents on either the phenyl ring (complex 3), pyridyl ring (2) or both rings (1) of the

Department of Chemistry, University of Warwick, Coventry, UK.

Electronic Supplementary Information (ESI) available: [details of any supplementary information available should be included here]. See DOI: 10.1039/x0xx00000x

chelated phenylpyridine ligand, **Figure 1**. The aldehyde group can form a covalent imine (Schiff base) adduct with an amine (e.g. Lys or N-terminal amino group). We sought to not only identify the specific sites of iridium binding to the peptides and the rest of the bound ligands, but also to distinguish between direct coordination of amino acid side-chains to Ir(III) and the formation of covalent bonds through condensation reactions involving the aldehyde functional group on the chelated ligand.

Methylated-cyclopentadienyl iridium compounds have been studied previously by MS and MS/MS by Qi et.al.¹⁴ However, in the present case, a new functional group (an aldehyde) was introduced into the C₅N-chelated ligand which allows the possibility of binding to potential cellular targets not only via the active metal centre (a common binding site for transition metal anticancer complexes), but also to react with the ligand functional groups and produce new additional covalent bonds. This enhanced reactivity has potential to produce interesting new reaction pathways and products modified by both covalent ligand-binding and coordination to the metal centre. Characterization of such products presents challenges to MS and especially MS/MS analysis, with the iridium complex having a dramatic effect on both threshold-based dissociations (such as CAD and IRMPD) and electron-based dissociations (such as ECD).

Experimental:

Substance P, [Lys]3-Bombesin, and formic acid were purchased from Sigma Aldrich (St. Louis, MO). LCMS grade Acetonitrile (ACN) was obtained from VWR (Radnor, PA) and used without further purification. Low concentration tuning mix was purchased from Agilent Technologies (Santa Clara, CA) and used as received. The iridium(III) anticancer complexes **Ir2+Cl** and **Ir3+Cl** were synthesised and characterised using previous methods.¹³ The synthesis of the di-aldehyde derivative (**Ir1+Cl**) is described in the Supporting Information (SI).

Reaction of Peptides with Iridium metallodrugs:

Aqueous solutions of Substance P (1 mM) and [Lysine]³-Bombesin (1 mM) were prepared and mixed with a solution of an iridium complex in ACN (250 μM) to give solutions of 0.5:1 and 1:1 (drug:peptide) mol ratio. The samples were then placed in an incubator (Genlab, Cheshire, UK) at 37 °C for 1-4 days before being diluted 50-fold with ACN to MS concentrations (~2.5 μM summed concentration for all reaction products) and frozen at -80 °C ready for MS analysis. Freshly prepared samples were compared to those frozen for 1 week to several months and showed no observable variation in their mass spectra. Frozen samples were thawed and placed on a multi vortexer (Grant Bio, Cambridge, UK) prior to MS analysis. No significant changes were observed for incubations longer than 1 day, as a result all data shown are from 1-day incubations.

FT-ICR Mass spectrometry:

Nano-electrospray (nESI) mass spectrometry was performed on a Bruker Solarix Fourier Transform Ion Cyclotron Resonance Mass Spectrometer (FT-ICR MS) fitted with a home-built nano electrospray ionisation (nESI) source and a 12 Tesla actively shielded magnet (Bruker Daltonics, Bremen, Germany). Aqueous peptide samples (5 μM) were spiked with 0.3% formic acid to aid effective ionisation during nESI. Iridium-containing samples were sprayed in ~99% ACN 1% H₂O (v/v after dilution) with no added acid.

For CAD MS/MS analysis; species of interest were isolated in the first quadrupole and accelerated into the hexapole collision cell for Collisionally Activated Dissociation (CAD) at 10-30 V and continuously accumulated for 0.1 - 4 seconds before transfer to the Infinity Cell for detection.¹⁶

For ECD MS/MS analysis; the species of interest were isolated in the first quadrupole, externally accumulated in the collision cell for 0.1-7 seconds and then transferred to the Infinity Cell for Electron Capture Dissociation (ECD) fragmentation and detection. Ions in the Infinity Cell were irradiated with 1.3 eV (peptides) - 2.5 eV (Ir adducts) electrons from a 1.5 A hollow cathode dispenser for 50 - 1200 ms prior to detection. Certain iridium-bound biomolecule species were also irradiated with a continuous wave IR laser (10.6 μm, Synrad Inc., Washington, USA) during the ECD event to aid in ECD fragmentation, but tuned to avoid any IR-induced fragmentation, spectra are marked accordingly in the SI.

MS/MS spectra were internally calibrated using the minimal number of unmodified (peptide spectra) or modified (Ir adduct spectra) b/c ions and the charge reduced species [M+nH]ⁿ⁻¹⁺ where possible (species used for calibration are marked). All assignments are available in the Supporting Information, **Tables ST2-ST13**.

Results and discussion:

The iridium complexes reacted readily with the Substance P (SubP) and [Lysine]³-Bombesin (L3BBS). The resulting spectra (**Figure 2**, and SI **Figure SF2**) show only a few species: unreacted Iridium complex+solvent adducts (minus the Cl ligand, lost during the ESI process), unreacted peptide species, and iridium-modified peptides. Iridium-containing species were readily assigned as such due to Iridium's characteristic isotope pattern (**Figure 2 inset**).¹⁷ The Ir complex+Substance P mass spectra all showed a single iridium-containing species as a result of the reaction. This species corresponded to the mass of the iridium complex+peptide minus the mass of a water molecule (hereafter referred to as the condensation product, [SubP+Irx-H₂O+H]²⁺). The amidated Substance P used in this study contains no amino acid group which would readily lose a water molecule, and no water loss, amine loss, or deamidation was observed for peptide-only control samples. As a result, the observed reaction product can arise from a condensation reaction with one of the aldehyde functional groups contained within the iridium ligand.

The mass spectra from the reaction of Ir complex+L3BBS peptide showed similar reaction products as the Ir complex+Substance P reaction: unmodified complex + adducts, unmodified peptide species, and a condensation product ($[\text{Ir drug}+\text{L3BBS}-\text{H}_2\text{O}+\text{H}]^{2+}$). For **Ir1**, the spectra also showed an additional reaction product, that of a non-condensation product, $[\text{Ir drug}+\text{L3BBS}+\text{H}]^{2+}$, based on observation of both the Ir complex without the Cl ligand and water/solvent molecule addition, ($[\text{IrC}_{10}\text{H}_{15}\text{C}_{10}\text{H}_6\text{N}_2]^+$ and $[\text{IrC}_{10}\text{H}_{15}\text{C}_{10}\text{H}_6\text{N}_2+\text{H}_2\text{O}]^+$, respectively, **Figure 2 inset**). The identity of the iridium complex modification for L3BBS species was ambiguous; even with accurate mass-mass spectrometry (readily achieved on the FT-ICR MS used). The two product species had exactly the same mass and only varied by the location of the H_2O . Both Collisionally Activated Dissociation (CAD) and Electron Capture Dissociation (ECD) were conducted on all iridium-modified species in order to elucidate not only the identity of the bound iridium complex, but also to locate the preferential binding sites for these novel therapeutic agents. It is noteworthy that after a 24 hour incubation with the iridium complexes, Substance P peptide had reacted nearly completely, giving a single reaction product. Although reaction with L3BBS produced two distinct reaction products for each Iridium complex, the extent of reaction was much lower (as observed by the lower relative intensity of peaks in the Ir-L3BBS spectra, **Figure 2**).

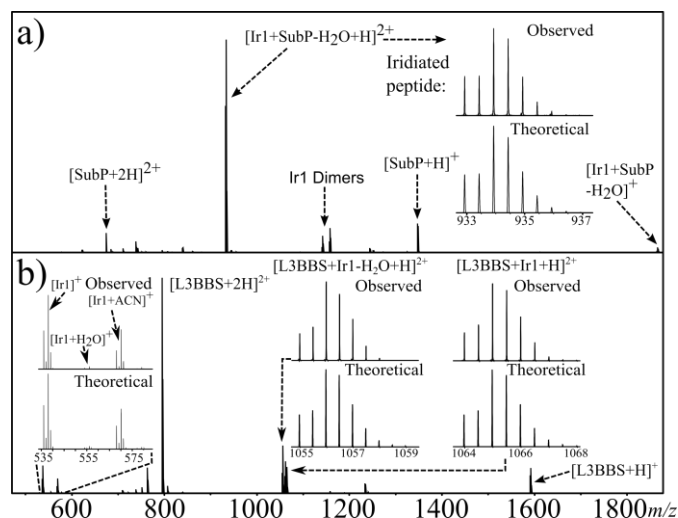


Figure 2: (a) Reaction of Substance P with iridium complex Ir1. (b) Reaction of [Lys]3-Bombesin with Ir1. Insets show the isotopic distributions for Ir1 and Ir1+peptide complexes.

Tandem MS of iridium-modified species

Previous studies of piano-stool iridium compounds binding to peptides by Qi *et al.* showed that the non-aldehyde functionalised analogues bind to methionine residues, and can be studied effectively using both CAD and ECD MS/MS.¹⁸ Many peptide and protein modifications, be they natural post translational modifications (PTM's) such as phosphorylation, synthetic modifications, or metal-based modifications, are often easily lost using dissociation techniques based on slow-heating/threshold (such as CAD), but can be retained using

electron-based dissociation techniques such as ECD, with metal complex modifications being particularly susceptible to loss during CAD.^{8,15,19} However, standard CAD and ECD MS/MS of the reaction products shown in **Figure 2** provided interesting results and non-standard dissociation mechanisms compared to the unmodified peptide species, each of which are detailed below.

The reactions of iridium complexes with Substance P showed only one iridiated-peptide product ($[\text{Ir}+\text{SubP}-\text{H}_2\text{O}+\text{H}]^{2+}$). The subsequent MS/MS spectrum of the quadrupole-isolated species is shown in **Figure 3**, below for ECD of **Ir1** and **SF9** and **14** for **Ir2** and **Ir3** respectively.

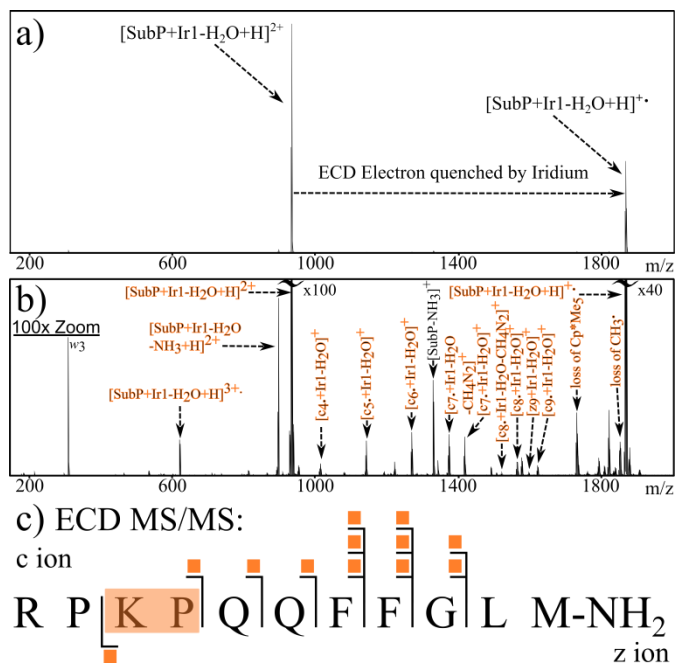


Figure 3: (a) Electron capture dissociation for the $[\text{SubstanceP}+\text{Ir1}-\text{H}_2\text{O}]^{2+}$ condensation product. (b) Vertical expansion (100x) of the spectrum (a) showing low intensity fragments. (c) Fragmentation map summarising assigned fragments. Orange squares/labels indicate assigned fragments containing the Ir modification.

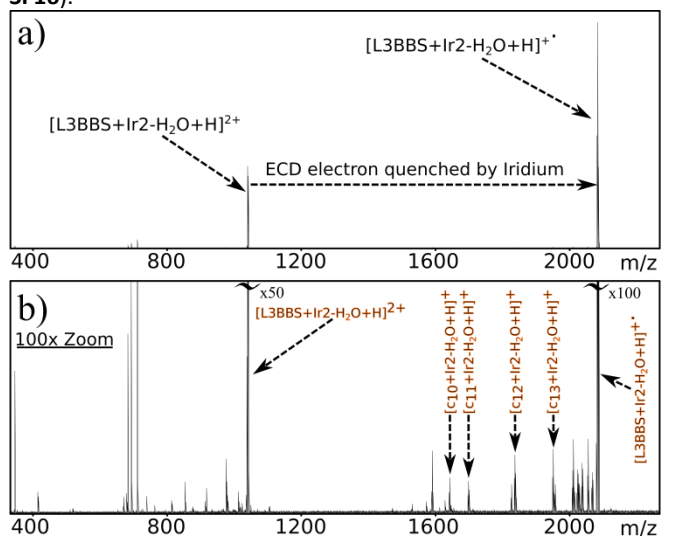
The iridium modified peptides required very different electron energies and pulse lengths to achieve both effective electron capture and ECD MS/MS compared to the corresponding unmodified peptide ions (~2-2.5 eV and 1.2 s vs. ~1-1.4 eV and 0.2 s respectively), with many energies simply producing electron capture, but little fragmentation. In addition, the intensity ratio of parent ion to charge-reduced species was drastically different between the pure peptide and Ir-modified-peptide ECD spectra. For instance; Substance P ECD MS/MS shows very effective electron capture, resulting in a charge-reduced species (CRS, e.g. $[\text{SubstanceP}+2\text{H}]^+$) ~5-10% intensity of the parent ion ($[\text{SubstanceP}+2\text{H}]^{2+}$) and good intensity ECD fragments (~10-25% of parent ion intensity).²⁰ For the iridium-modified Substance P, the intensity of the CRS compared to the 2+ parent ion was 41%, which is unusually high for peptide ECD MS/MS. The resulting ECD fragments were also of very low intensity ($\leq 1\%$) compared to unmodified

Substance P ECD MS/MS, indicating that the iridium modification has a dramatic effect upon the ECD process. The Iridium within the complex was in the 3+ oxidation state (i.e. Ir^{III} with two charges neutralised via bonds to ligands (Cp^*Me_5^- and the NC^- ligand), leaving the Iridium centre with an overall 1+ charge, which explains why the addition of only a single proton to produce the $[\text{Peptide}+\text{Ir}+\text{H}]^{2+}$ species was detected. The $[\text{Ir}]^+$ centre can be easily reduced to $[\text{Ir}]^0$ by electron capture during ECD MS/MS to produce a charge-reduced species in which the electron has been quenched effectively by the iridium centre, rather than a more typical CRS where the electron causes backbone/sidechain dissociation, with the individual fragments remaining bound together via hydrogen bonds/other covalent/backbone bonds.^{21,22}

The quenching of electrons during electron-based dissociations has been observed before when studying covalently-bound heme-containing biomolecules, such as cytochrome c,²³ and species with particularly high histidine content. The conjugated π -systems were believed to stabilise incoming electrons and the resulting radical species generated, preventing/subduing ECD/ETD fragmentation during MS/MS.²⁴ Europium-bound biomolecules and some other heavy metal adducts are also believed to be so-called “electron sinks” and quench electrons.²⁵ However these effects have been observed only with heptadentate ligands surrounding the metal centre or with bare metal centres as adducts/charge carriers on other species and not as specific biomolecule modifications as observed for metal complexes. Interesting contributions from Asakawa et al. have shown how the properties of various metals affect electron capture during electron transfer dissociation (ETD), and how this may be exploited for enhanced sequencing of target biomolecules.^{26,27}

Despite the partial quenching of ECD electrons by iridium, low intensity fragments were observed in all ECD MS/MS spectra of Ir-containing reaction products (Figure 3+4, SI Figures SF5, SF7, SF15, and SF17). These fragments are summarised in the corresponding fragmentation maps (Figure 3, SF6, SF7, SF13, SF15, and SF17) and SI Tables ST2, ST3, ST4, ST8, ST10, and ST12). For the Iridium complex-modified Substance P species, the data suggest a preference for lysine binding, accompanied by loss of a water molecule during the process, indicating a condensation reaction between the terminal primary amine on the lysine side chain and the aldehyde functional group present on the bidentate ligand within the iridium complex. The condensation reaction between the complex and the biomolecule results in the formation of an imine, a strong covalent bond which does not involve the metal centre directly. Also, surprisingly, there seems to be no evidence of binding of Iridium to the terminal methionine residue of either peptide, in contrast to previous studies by Qi *et al.*,¹⁸ who showed that the non-aldehyde functionalised iridium(III) complexes bind strongly to methionine residues in the calcium-binding protein calmodulin. The presence of the aldehyde functional group(s) appear to influence both the mechanism of binding (binding via the ligand rather than the metal centre) and the preferential location of binding (lysine over methionine).

ECD MS/MS of the $\text{Ir}_x+\text{L3BBS}$ condensation products ($x=1, 2$, or 3) (Figure 4, below, and SI Figures SF5, SF7, SF15, and SF17) also showed an unusually high CRS relative intensity compared to the parent ion ($\sim 250\%$), showing extensive quenching of ECD electrons. ECD of the unmodified L3BBS was fairly typical, with a CRS intensity $\sim 10\text{--}20\%$ compared to that of the precursor. ECD MS/MS analysis of the iridium-modified peptides was hindered greatly by electron quenching at the iridium centre, and only a few fragments could be assigned, indicating Iridium binding towards the N-terminus of the peptide (*vide infra*). Fortunately due to the covalent linkage, CAD MS/MS was able to sequence these species effectively and assign binding of the complexes to the lysine of the peptides via an imine linkage (SI SF8, SF9, SF11, SF14, and SF16).



c) ECD MS/MS:



Figure 4: (a) IRECD MS/MS electron capture by the [Lys]3-Bombesin+Ir2-H₂O condensation product ($[\text{L3BBS}+\text{Ir2-H}_2\text{O}+\text{H}]^{2+}$). (b) Vertical expansion (100x) of the spectrum (a) showing low intensity fragments. (c) Fragmentation map summarising assigned fragments. Shaded squares/labels indicate assigned fragments containing the Ir modification.

ECD MS/MS of the non-condensation product ($[\text{Ir}_2+\text{L3BBS}+\text{H}]^{2+}$) are shown in Figure 5 and in the SI (SF13 and ST8). The iridium complex bound to the peptide was shown to have a drastic effect on the ECD spectrum, with the main fragmentation pathway appearing to be electron capture at the iridium centre (as seen in the condensation product ECD spectrum). The reduction of the iridium centre by captured electrons caused the complex to dissociate from the biomolecule and produce a large peak corresponding to unmodified $[\text{L3BBS}+\text{H}]^+$ being a 1+ ion, the $[\text{L3BBS}+\text{H}]^+$ species produced was not able to undergo further ECD MS/MS fragmentation and produce detectable fragments due to the

charge being neutralized upon electron capture. Although most of the precursor ions fragmented via loss of the Iridium complex modification, low intensity fragment ions were observed and were used to locate the modification binding site. The iridium complexes were shown to bind preferentially to the His-11 residue within L3BBS in a non-condensation (i.e. metal-centred) fashion via a dative covalent bond to the Ir centre.

The detection of histidine-centred binding to Ir showed a change in the binding preference of these functionalised Iridium compounds in contrast to the unfunctionalised ligand Iridium(III) compounds studied previously¹⁸ which showed a preference for methionine residues and for the condensation products described above in preference to Lysine residues. Many other transition metal complexes, especially those based upon platinum(II), have often shown a distinct preference for binding at sulphur-containing residues (Met, Cys^{4,28,29}). In addition it has been reported that even some iridium(III) compounds also preferentially bind to methionine residues. However the results obtained here clearly highlight the fact that the behaviour and reactivity of metal-based complexes varies greatly depending on the metal-bound ligands and the available biomolecule functional groups.

Relatively small changes to ligand configuration/identity can affect the course of reactions, as shown above as the aldehyde functionality and not only change the mechanism of binding to biomolecules, but also the preferred metal binding site from methionine (as shown by Qi et.al.)¹⁸ to histidine (shown herein).

The formation of the covalent imine bond by condensation suggested that the iridium-peptide modification should survive (even partially) a threshold-based dissociation technique. CAD MS/MS was conducted on the condensation and non-condensation reaction products observed in the L3BBS spectrum. As expected CAD of the non-condensation (Ir-bound) product resulted in loss of the iridium modification at low CAD energies/voltages (~5-8V) whereas backbone fragmentation did not occur to a useful (sequence informative) extent without the use of high voltages (15-20V). CAD MS/MS of the L3BBS condensation products, on the other hand, was very successful (SI Figure SF8, SF9, SF11, SF14, and SF16). Though CAD caused some loss of the bidentate ligand from the CRS, this was a minor fragmentation pathway. The vast majority of peaks observed were readily assigned to unmodified/iridium-modified b/y fragments and side-chain loss ions therefrom. The CAD MS/MS provided correlating and complementary data to the ECD MS/MS of the condensation product, summarised in the fragmentation maps. The complexes clearly bind preferentially to the lysine residue, via condensation and loss of a water molecule.

Although the **Ir1** complex contained two aldehyde functional groups within the bidentate ligand, no cross-linked, di-condensation product was observed (i.e. a product formed from separate condensation reactions, one at each aldehyde group), even during subsequent experiments using higher ratios of **Ir1** to peptide, nor with longer reaction times (up to 7

days). This lack of further reaction suggests a difference in reactivity between the aldehyde groups on the phenyl and pyridine rings. Comparisons between spectra of **Ir2**+peptide and **Ir3**-peptide showed that regardless of which ring the aldehyde group is positioned; only one condensation reaction occurs (**SF2**), indicating that another factor inhibits binding once the first imine bond is formed – most likely steric hindrance from the peptide coiling around/blocking further access to areas of the metal complex post-imine formation.

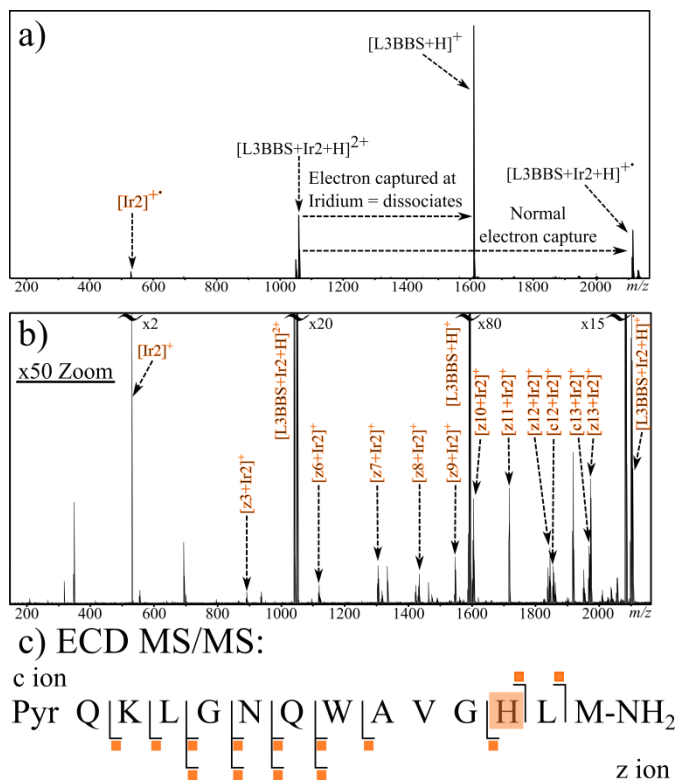


Figure 5: (a) ECD MS/MS spectrum of the [Lys]³-Bombesin+**Ir2** reaction product ([L3BBS+**Ir2**+H]²⁺). (b) Vertical expansion (50x) of the spectrum (a) showing low intensity fragments. (c) Fragmentation map summarising assigned fragments. Shaded squares/labels indicate assigned fragments containing the Ir modification.

A low intensity peak was detected in the mass spectrum of the **Ir1**+L3BBS reaction mixture corresponding to a possible cross-linked **Ir1**+peptide species ([**Ir1**+2xL3BBS-H₂O+2H]³⁺). However, a peptide dimer peak ([2xL3BBS+3H]³⁺) was also observed – resulting from 2 peptide ions held together via non-covalent interactions (such as hydrogen bonds). Since both the peptide dimer and an **Ir1**-modified species containing two peptides were both observed, the identity of the **Ir1**-modified species was ambiguous. Possible species include a crosslinked peptide (resulting from imine formation and Ir binding) or an L3BBS dimer modified at one lysine residue (as described above). CAD and ECD MS/MS were carried out on the possible dimer species. CAD MS/MS predictably caused dissociation of the dimer at low CAD voltages (as discussed above), and little information was obtained other than typical lysine-modified fragments (as observed in the CAD MS/MS of

the individual condensation products). ECD MS/MS was hindered greatly by electron-quenching at the iridium centre which resulted in very low intensity fragments and the loss of the iridium complex formed from the most abundant fragmentation channel. Few sequence-informative fragments were identified, but those that were, showed correlating information to that of the ECD MS/MS of individual modified peptides. The metal complex was found to bind via an imine linkage to the lysine residue and to the other peptide via a coordination bond to the histidine residue. This indicates that the species was in fact an iridium cross-linked reaction product (**Figure 6**, below). Similar Iridium cross-linked products were also observed in the **Ir2**+L3BBS and **Ir3**+L3BBS mass spectra, again re-enforcing that only one aldehyde group and one metal-centred bond are required for crosslinking using these iridium(III) complexes. The Substance P+**Ir1**/**Ir2**/**Ir3** spectra did not show any evidence of iridium-cross-linking, despite the availability of a methionine residue and the presence of two reactive aldehyde groups on the **Ir1** complex.

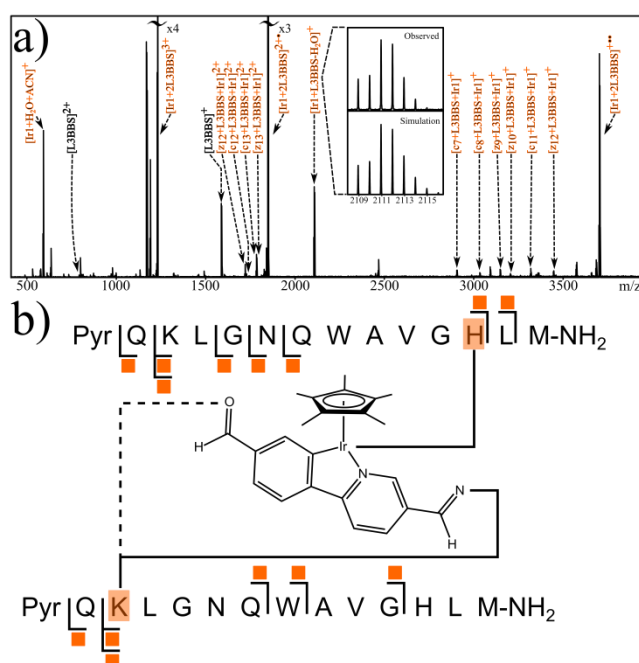


Figure 6: ECD MS/MS spectrum of the $[\text{Ir1}+2\text{xL3BBS-H}_2\text{O}+2\text{H}]^{3+}$ species (a) and corresponding fragmentation map (b) showing the species cross-linked via the iridium metallodrug via an imine linkage and an iridium co-ordination bond.

Conclusions:

Aldehyde-functionalised iridium piano-stool (half-sandwich) Cp^* compounds were shown to bind to peptides via a coordination bond between the iridium metal centre and histidine residues when available (**Figure 7**). CAD MS/MS studies of Ir-bound species resulted in loss of the metal-based modification and subsequent secondary fragmentation of the resulting unmodified peptide, losing all sequence informative-fragments related to the location of the modification.

Metallodrug	Peptide	Product	MS/MS	Peptide cleavage map
Ir1	SubP	Condensation	ECD	R P K P Q L F F G L M-NH ₂
	L3BBS	Condensation	IRECD	Pyr Q K L G N Q W A V G H L M-NH ₂
			CAD	Pyr Q K L G N Q W A V G H L M-NH ₂
		Non-condensation	ECD	Pyr Q K L G N Q W A V G H L M-NH ₂
Ir2	SubP	Condensation	CAD	R P K P Q Q F F G L M-NH ₂
	L3BBS	Condensation	IRECD	Pyr Q K L G N Q W A V G H L M-NH ₂
			CAD	Pyr Q K L G N Q W A V G H L M-NH ₂
		Non-condensation	ECD	Pyr Q K L G N Q W A V G H L M-NH ₂
Ir3	SubP	Condensation	CAD	R P K P Q Q F F G L M-NH ₂
	L3BBS	Condensation	IRECD	Pyr Q K L G N Q W A V G H L M-NH ₂
			CAD	Pyr Q K L G N Q W A V G H L M-NH ₂
		Non-condensation	ECD	Pyr Q K L G N Q W A V G H L M-NH ₂

Figure 7: Summary of the various metallodrug-peptide reaction products observed and studied using different MS/MS techniques, along with corresponding peptide cleavage maps.

ECD MS/MS of the coordinative-covalently bound species was especially challenging due to the electron-quenching effect of the iridium based modification, but did produce fragments revealing the locations of the modifications. These functionalised iridium compounds were shown to bind to lysine residues within biomolecules via condensation reactions, creating a covalent imine linkage. CAD MS/MS of the imine species was very effective, with the iridium modification being retained in subsequent fragments and allowing determination of the location of the modification site. Again ECD MS/MS of the imine-containing species was hindered greatly by the electron-quenching iridium centre, but sequence-informative fragments were observable and in some cases were critical in locating and characterising Ir-based modifications formed by covalent modification of lysine residues.

The work reinforces the need to use complimentary MS/MS techniques in order to study new metallo-peptide systems effectively and accurately. In addition, the chemistry of biomolecule modifications can affect MS and MS/MS behaviour drastically. The mode of use of slow heating techniques (such as CAD) and electron-based techniques differ greatly, with electron-based techniques such as ECD requiring careful tuning of electron energies, but enabling new fragmentation pathways and revealing sequence information.

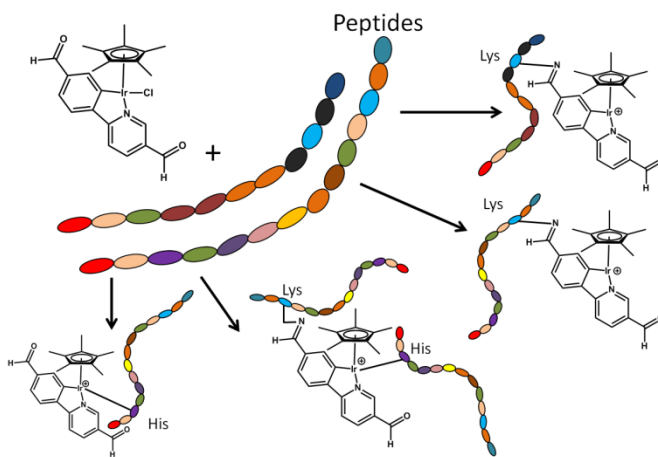
Although quenching of electrons by iridium modifications was encountered at many electron energies, effective ECD fragmentation was viable with careful tuning (<0.1 eV increments) and balancing of ICR cell parameters, enabling electron capture at other points within the modified peptide structures. Combinations of complementary MS/MS techniques are key to characterising challenging metallodrug-peptide systems, both natural and modified.

Acknowledgements:

We thank the EPSRC (Warwick Centre for Analytical Science (grant no. EP/F034210/1, EP/J000302, J003022/1, N021630/1, and N033191/1), the European Research Council (grant no.247450), Biotechnology and Biological Sciences Research Council (grant no. P021875/1), Bruker Daltonics, and Warwick Collaborative Postgraduate Research Scholarships (WCPRS) for funding.

References:

- 1 J. Reedijk, *Chem. Rev.*, 1999, **99**, 2499–2510.
- 2 H. Li, S. A. Wells, J. E. Jimenez-Roldan, R. A. Römer, Y. Zhao, P. J. Sadler and P. B. O'Connor, *Protein Sci.*, 2012, **21**, 1269–79.
- 3 H. Li, J. R. Snelling, M. P. Barrow, J. H. Scrivens, P. J. Sadler and P. B. O'Connor, *J. Am. Soc. Mass Spectrom.*, 2014, **25**, 1217–1227.
- 4 H. Li, T. Lin, S. L. Van Orden, Y. Zhao, M. P. Barrow, A. M. Pizarro, Y. Qi, P. J. Sadler and P. B. O'Connor, *Anal. Chem.*, 2011, 9507–9515.
- 5 Z. Xu, J. B. Shaw and J. S. Brodbelt, *J. Am. Soc. Mass Spectrom.*, 2013, **24**, 265–73.
- 6 B. Sirichanchuen, T. Pengsuparp and P. Chanvorachote, *Mol. Cell. Biochem.*, 2012, **364**, 11–18.
- 7 S. H. van Rijt, I. Romero-Canelón, Y. Fu, S. D. Shnyder and P. J. Sadler, *Metallomics*, 2014, **6**, 1014.
- 8 C. A. Wootton, C. Sanchez-Cano, A. F. Lopez-Clavijo, E. Shaili, M. P. Barrow, P. J. Sadler and P. B. O'Connor, *Chem. Sci.*, 2018, **9**, 2733–2739.
- 9 J. J. Soldevila-Barreda, I. Romero-Canelón, A. Habtemariam and P. J. Sadler, *Nat. Commun.*, 2015, **6**, 6582.
- 10 W. H. Ang, A. Casini, G. Sava and P. J. Dyson, *J. Organomet. Chem.*, 2011, **696**, 989–998.
- 11 K. S. Lovejoy and S. J. Lippard, *Dalton Trans.*, 2009, 10651–9.
- 12 S. Banerjee, J. J. Soldevila-Barreda, J. A. Wolny, C. A. Wootton, A. Habtemariam and I. Romero-Canelon, *Chem. Sci.*, 2018, **9**, 3177–3185.
- 13 A. J. Millett, A. Habtemariam, I. Romero-Canelón, G. J. Clarkson and P. J. Sadler, *Organometallics*, 2015, **34**, 2683–2694.
- 14 Z. Liu and P. J. Sadler, *Acc. Chem. Res.*, 2014, **47**, 1174–1185.
- 15 C. A. Wootton, C. Sanchez-Cano, H.-K. Liu, M. P. Barrow, P. J. Sadler and P. B. O'Connor, *Dalt. Trans.*, 2015, **44**, 3624–3632.
- 16 P. Caravatti and M. Allemann, *Org. Mass Spectrom.*, 1991, **26**.
- 17 C. A. Wootton, Y. P. Y. Lam, M. Willetts, M. A. van Agthoven, M. P. Barrow, P. J. Sadler and P. B. O'Connor, *Analyst*, 2017, **142**, 2029–2037.
- 18 Y. Qi, Z. Liu, H. Li, P. J. Sadler and P. B. O'Connor, *Rapid Commun. Mass Spectrom.*, 2013, **27**, 2028–32.
- 19 S. M. M. Sweet, C. M. Bailey, D. L. Cunningham, J. K. Heath and H. J. Cooper, *Mol. Cell. Proteomics*, 2009, **8**, 904–12.
- 20 A. F. Lopez-Clavijo, M. P. Barrow, N. Rabbani, P. J. Thornalley and P. B. O'Connor, *Anal. Chem.*, 2012, **84**, 10568–75.
- 21 J. Simons, *J. Am. Chem. Soc.*, 2010, **132**, 7074–85.
- 22 J. Simons, *Chem. Phys. Lett.*, 2010, **484**, 81–95.
- 23 K. Breuker, S. Brüsweiler and M. Tollinger, *Angew. Chemie - Int. Ed.*, 2011, **50**, 873–877.
- 24 T. W. Chung, C. L. Moss, J. A. Wyer, A. Ehlerding, A. I. S. Holm, H. Zettergren, S. B. Nielsen, P. Hvelplund, J. Chamorro-rooke and B. Bythell, 2010, 10728–10740.
- 25 J. Mosely, B. Murray and D. Parker, *Eur. J. Mass Spectrom.*, 2009, **15**, 145–155.
- 26 D. Asakawa and I. Osaka, *Anal. Chem.*, 2016, **88**, 12393–12402.
- 27 D. Asakawa, A. Miyazato, F. Rosu and V. Gabelica, *Phys. Chem. Chem. Phys.*, 2018, **20**, 26597–26607.
- 28 H. Li, Y. Zhao, H. I. A. Phillips, Y. Qi, T.-Y. Lin, P. J. Sadler and P. B. O'Connor, *Anal. Chem.*, 2011, **83**, 5369–76.
- 29 N. Zhang, Y. Du, M. Cui, J. Xing, Z. Liu and S. Liu, *Anal. Chem.*, 2012, **84**, 6206–12.



TOC graphic